A HYBRID ALGORITHM BASED ON K-L EXPANSION AND INTERVAL ANALYSIS METHOD FOR DYNAMIC LOAD OF BRIDGE - VEHICLE INTERACTION SYSTEM WITH UNCERTAINTY

TRUONG VAN HUY[1], TRUONG QUANG VINH[1], CHAU MINH QUANG[2*]

[1]*Faculty of Technology, IUH Quang Ngai Campus, Industrial University of Ho Chi Minh City*

[2]*Institute of International and Postgraduate Education, Industrial University of Ho Chi Minh City*

[*]*Corresponding Author: chauminhquang@iuh.edu.vn*

DOIs: https://www.doi.org/10.46242/jstiuh.v75i3.5183

ABSTRACT

Dynamic load identification of bridge - vehicle- interaction system on uncertain parameters is studied in this paper. The vehicle is modeled by a two degrees of freedom mass-spring system and the bridge is modeled as an Euler-Bernoulli beam. A hybrid method that combines the Karhunen-Loève expansion and the interval analysis method is proposed to determine the midpoint value, lower and upper bounds of dynamic load acting on the vehicle-bridge system with uncertainty. The road surface roughness and excitation force of the bridge, which are assumed as Gaussian random processes, are described by the Karhunen–Loève expansion. Uncertain parameters of the structure are considered as interval variables, due to the fact that only their bounds are needed. The moving load identification algorithm can be formulated into an computational inverse problem. To prove the results obtained by proposed method HKIM, the interval analysis method (IAM) is also implemented. The results obtained by proposed method are effective for dynamic load of system with uncertainty.

Keywords: Load identification; inverse problem; Karhunen–Loe've expansion; interval analysis; hybrid method.

1. INTRODUCTION

In the past several decades, investigations on dynamic responses of bridge - vehicle interaction system has attracted more and more attractions. In order to deep understand the mechanism, various vehicle-bridge models have been developed, and the most commonly used models are the quarter car model [1,2], half car model [3], tractor-trailer model [4] and three-dimensional vehicle model [5,6]. Among these models, three-dimensional vehicle model is capable of modeling more complex in the force problem of bridge - vehicle interaction system.

Due to its importances, lots of researches are focused on dynamic response analysis of bridge – vehicle interaction system. Henchi [7] proposed an algorithm for evaluating the dynamics of a bridge decomposed into finite elements of three-dimensional with a traffic flow running on the bridge crest at a specified speed. The loads acting into the bridge deck are modeled as nodal forces using finite element (FE) functions. The combined equations of motion of the bridge-vehicle system are solved directly without using iterations [8].

A random force recognition algorithm is proposed to measure the statistics of the applied forces from random samples of the bridge deck. The random vibration of bridge structures under moving loads has been studied by Zibdeh [9]. This problem has also been studied for application in the stochastic analysis of bridge-vehicle interaction systems such as Law [10]. Law [11,12,13] also presented a identification model of moving load based on finite element, condensation technique. The displacements are considered as the shapes functions of the FE and the measured responses may be limited to a very small of principal degrees of freedom of the bridge system..

Wu [14] propose an approach to determine dynamic loads based on the Karhunen–Loève extension (KLE). The mathematical of the bridge - vehicle is formulated by using the FE in which the Gaussian are represented by the KLE. Both system parameters and applied forces are simulated to be fitted for Gaussian random processes. Jiang et al. Jiang et al. [15] suggested an optimization method for uncertain structures based on convex model and a satisfaction degree of the interval. Convex model is used to describe the uncertainty in which the intervals of the uncertain parameters are considered. Jiang et at [16,17,18,19] also proposed a method to solve uncertain structural problem based on a nonlinear interval number programming and an interval analysis method. Based on an order relation of interval mathematics, the uncertain optimization problem is transformed to calculate the values of the objective function. Liu et al. Liu et al. [20] and Liu et al. [21] suggested interval analysis method to deal uncertainty based on the inverse problem which is a class of inverse problem in the system parameters of structure with uncertainty. These methods are developed an efficient uncertainty optimization algorithm.

The dynamic behavior of a bridge under moving traffic with limited but uncertain system parameters was studied by Liu [22]. The calculation formulas for the midpoint, span width, lower and upper limits of the vertical action of the bridge are improved using the method of modal superposition and span operations. In which, the LHNPSO algorithm improved from PSO is applied to determine the lower and upper limits of the dynamic response. N. Liu et al. [23] also proposed a random interval moment model to analysis of the bridge - vehicle interaction system. The study analyzes the hybrid probability interval dynamics of the bridge - vehicle interaction with a mixture of random and interval attributes. Meanwhile, the parameters of vehicle are interval variables and the parameters of bridge are random variables. N. Liu et al. [30] proposed the hybrid probabilistic interval dynamic analysis of vehicle–bridge interaction system with a mixture of random and interval properties. The vehicle's parameters are considered as interval variables and the bridge's parameters are treated as random variables. N. Liu et al. [31] proposed interval dynamic response analysis of vehicle-bridge interaction system with uncertain parameters. The bridge's and vehicle's parameters are considered as interval variables. A half-car model is used to represent a moving vehicle and the bridge is assumed as a simply supported Euler–Bernoulli beam. P. H. Ni et al. [32] proposed a reliability-based design optimization method for bridge structures, considering the uncertainties of the material parameters and the effect of bridge-vehicle interaction.

In this paper, a hybrid method that combines the K-L expansion and interval analysis model is proposed to determine the lower and upper bounds of dynamic load acting on uncertain structures. The vehicle is modeled by a two degrees of freedom mass-spring model and the bridge is modeled as an Euler-Bernoulli beam. The road surface roughness and excitation force, which are assumed as Gaussia, are computed by the Karhunen–Loève. Load algorithm can be formulated by inverse problem. The bounds of load identification calculated based on the interval analysis method in which the uncertain parameters of system are considered as interval variables. The effectiveness of this method is demonstrated in Section numerical simulation.

The remainder of this paper is organized as: Section 2 presents the model and the equation of motion of vehicle-bridge system. Section 3 presents a brief introduction of the Karhunen–Loève expansion model. The road surface roughness is presented in Section 4. Section 5 presents load identification algorithm based on the inverse problem and interval analysis. Numerical simulation and results are given in Section 6. Final, conclusion is stated in the Section 7.

2. MODELING OF THE VEHICLE-BRIDGE SYSTEM

2.1 The equation of motion of vehicle-bridge system.

The bridge - vehicle model is simplified as shown in Fig.1. Bridge deck is reseached to determine the load bounds on the structure. The equation of motion of the vehicle-bridge in Fig.1 is expressed using the Lagrange formulation as followings [24]:

$$\rho\frac{\partial^2 y(x,t)}{\partial t^2}+C\frac{\partial y(x,t)}{\partial t}+EI\frac{\partial^4 y(x,t)}{\partial x^2}=P(t)\delta(x-vt) \tag{1}$$

The equation of motion of the vehicle can be rewritten in matrix form as:

$$\begin{bmatrix} M & 0 \\ 0 & m \end{bmatrix}\begin{Bmatrix} \ddot{z}_1(t) \\ \ddot{z}_2(t) \end{Bmatrix}+\begin{bmatrix} c_1 & -c_1 \\ -c_1 & c_1 \end{bmatrix}\begin{Bmatrix} \dot{z}_1(t) \\ \dot{z}_2(t) \end{Bmatrix}+\begin{bmatrix} k_1 & -k_1 \\ -k_1 & k_1 \end{bmatrix}\begin{Bmatrix} z_1(t) \\ z_2(t) \end{Bmatrix}=\begin{Bmatrix} 0 \\ P(t)-(M+m)g \end{Bmatrix} \tag{2}$$

where $y(x, t)$ is the bridge vertical. z_1, z_2 are the displacements of vehicle and wheel, respectively. k_1, c_1 are the stiffness and damping of the spring, k_2 is the stiffness of the tires. C, EI, ρ is the damping, bending stiffness and unit of mass per length of the bridge. $\delta(x-vt)$ is function evaluated the contact point at position $x= vt$, and v is the speed of vehicle. M, m are the masses of the vehicle body and the wheel, respectively. $P(t)$ is the contact force between the wheel and surface bridge, using the Hertz elastic contact model as

$$P(t)=\begin{cases} k_2(r-z_2-z_{20}-y(vt,t))^{3/2} \\ r-z_2-z_{20}-y(vt,t)\geq 0 \\ 0 \quad r-z_2\text{-}\,\mathrm{z}_{20}-y(vt,t)\leq 0 \end{cases} \tag{3}$$

where r is the roughness at the location of read. $z_{20}=-\left(\dfrac{m+M}{k_2}g\right)^{2/3}$ is the deformation of the spring under gravity load g.

2.2 Mode shapes of the bridge deck

The solution to Eq.(1), express the transverse displacement $y(x,t)$ in modal coordinates of the bridge:

$$y(x,t)=\sum_{i=1}^{\infty}\phi_i(x)q_i(t) \tag{4}$$

where $\phi_i(x)$, $q_i(t)$ are the mode shapes function of the ith mode and associated modal coordinates of the bridge.

For supported beam, the modal shapes of the bridge

$$\phi_i(x)=\sin\frac{i\pi x}{L} \tag{5}$$

Substitution Eq. (4) into Eq.(1), multiplying both sides of the equation by $\phi_n(x)$ and integrating with respect to x over the length of the beam, we obtain:

$$\rho\frac{d^2q_n(t)}{dt^2}\int_0^L\phi_n^2(x)dx+C\frac{dq_n(t)}{dt}\int_0^L\phi_n^2(x)dx+EIq_n(t)\int_0^L\phi_n(x)\frac{d^4\phi_n(x)}{dx^4}dx=\int_0^L\delta(x-vt)P(t)\phi_n(x)dx \tag{6}$$

where $$\phi_n(x)=\sin\frac{n\pi x}{L} \tag{7}$$

As bridge mass is more than the vehicle mass and the tire damping is not large, Eq.(6) can be simplified as:

$$\ddot{q}_n(t)+2\xi_n\omega_n\dot{q}_n(\mathrm{t})+\omega_n^2q_n(t)=\frac{2}{\rho L}P(t)\sin\frac{n\pi vt}{L} \tag{8}$$

In this paper, the Wilson's damping hypothesis is adopted as

$$c=2\rho\xi_n\omega_n \tag{9}$$

where ξ_n , ω_n are damping ratio and frequency of the nth vibration mode respectively,

with $$\omega_n=\frac{n^2\pi^2}{L^2}\sqrt{\frac{EI}{\rho}} \tag{10}$$

Via Eqs. (2)and Eq. (8) the equation of motion of the bridge - vehicle can be rewritten as:

$$\ddot{q}+C\dot{q}+Kq=F(t) \tag{11}$$

where $q=\{q_1\ q_2\ \cdots\ q_n\ z_1\ z_2\}^T$ is the displacement vector. $\dot{q}$, $\ddot{q}$ are the velocity vectors and acceleration, respectively. C and K are the damping and stiffness matrices of the bridge, which can be expressed as follows:

$$C=\begin{bmatrix} 0 & 0 & \cdots & 0 & 0 & 0 \\ 0 & 0 & \cdots & 0 & 0 & 0 \\ \cdots & \cdots & \cdots & \cdots & \cdots & \cdots \\ 0 & 0 & \cdots & 0 & 0 & 0 \\ 0 & 0 & \cdots & 0 & \frac{c_1}{M} & -\frac{c_1}{M} \\ 0 & 0 & \cdots & 0 & -\frac{c_1}{m} & \frac{c_1}{m} \end{bmatrix} \tag{12}$$

$$K=\begin{bmatrix} \frac{EI}{\rho}\left(\frac{\pi}{L}\right)^4 & 0 & \cdots & 0 & 0 & 0 \\ 0 & \frac{EI}{\rho}\left(\frac{2\pi}{L}\right)^4 & \cdots & 0 & 0 & 0 \\ \cdots & \cdots & \cdots & \cdots & \cdots & \cdots \\ 0 & 0 & \cdots & \frac{EI}{\rho}\left(\frac{n\pi}{L}\right)^4 & 0 & 0 \\ 0 & 0 & \cdots & 0 & \frac{k_1}{M} & -\frac{k_1}{M} \\ 0 & 0 & \cdots & 0 & -\frac{k_1}{m} & \frac{k_1}{m} \end{bmatrix} \tag{13}$$

$F(t)$ is the force vector, which is shown as:

$$F(t)=\left[P(t)\frac{2\phi_1(vt)}{\rho L} \ \ldots \ P(t)\frac{2\phi_n(vt)}{\rho L} \ \ 0 \ \ P(t)\text{-}mg\text{-}Mg\right]^T \tag{14}$$

3. KARHUNEN-LOE'VE EXPANSION

3.1 Theory

The KLE of a stochastic process $u(x,\theta)$ based on a bounded, symmetric, positive-definite variance function $C(x_1,x_2)$ with spectral analysis is as follows:

$$C(x_1,x_2)=\sum_{n=0}^{\infty}\beta_n\varphi_n(x_1)\varphi_n(x_2) \tag{15}$$

where β_n and φ_n are the eigenvalues and eigenvectors of the variance kernel, respectively.
hey can be shown to be solutions [25] of the following integration formula:

$$\int C(x_1,x_2)\varphi_n(x)dx_1=\beta_n\varphi_n(x_2) \tag{16}$$

Since the object is symmetric and the variance kernel has positive definiteness, its eigenvalues are orthogonal. Therefore, the eigenvectors can be normalized as follows:

$$\int \varphi_n(x)\varphi_m(x)dx=\delta_{nm} \tag{17}$$

where δ_{nm} is the Kronecker delta and

$$u(x,\theta)=\bar{u}(x)+\tilde{u}(x,\theta)=\bar{u}(x)+\sum_{n=1}^{\infty}\xi_n(\theta)\sqrt{\beta_n}\varphi_n(x) \tag{18}$$

where $\bar{u}(x),\xi_n(\theta)$ are denotes the expected value $u(x,\theta)$ and a set of random variables respectively. $\xi_n(\theta)$ can also be expressed as: [25]

$$\xi_n(\theta) = \frac{1}{\sqrt{\beta_n}} \int \tilde{u}(x,\theta)\varphi_n(x)dx \tag{19}$$

when $u(x,\theta)$ is a Gaussian, $\xi_n(\theta)$ will be a group of variables with as:

$$\begin{aligned} &E(\xi_n(\theta)) = 0 \\ &E(\xi_k(\theta)\xi_L(\theta)) = \delta_{kL} \end{aligned} \tag{20}$$

3.2 Representation of stochastic process vector

$V(t,\theta)$ is the stochastic process vector *m*-dimensional, which be defined as

$$V(t,\theta) = \{v_1(t,\theta)v_2(t,\theta)...v_m(t,\theta)\}^T \tag{21}$$

The mean of the *i*th element of $V(t,\theta)$ denoted as $\bar{v}_i(t)$ and $\tilde{v}_i(t,\theta)$ respectively as:

$$\bar{v}_i(t) = E(\bar{v}_i(t,\theta))(i = 1,\ldots,m) \tag{22}$$

$$\tilde{v}_i(t,\theta) = v_i(t,\theta) - \bar{v}_i(t)(i = 1,\ldots,m) \tag{23}$$

$V(t,\theta)$ can be discredited at the equal time step interval Δt, and $n = T/\Delta t + 1$ is the number of time instances, where T is the time. The KLE of the discrete vectors of stochastic can be obtained by reformulating the unrecognized vector into a dimensional VV as follows:

$$VV(t,\theta) = \{v_1(t_1,\theta)\ldots v_1(t_n,\theta)v_2(t_1,\theta)\ldots v_2(t_n,\theta)\ldots v_m(t_1,\theta)\ldots v_m(t_n,\theta)\}^T \tag{24}$$

$\Gamma_{vv.vv}$ is the covariance matrix, which can be defined as:

$$\Gamma_{vv.vv}(i,j) = E\{(v_i(t,\theta) - \bar{v}_i(t)(v_j(t,\theta) - \bar{v}_j(t))\} \tag{25}$$

and which can be written in matrix form as [1]

$$\Gamma_{vv.vv} = \begin{bmatrix} \Gamma_{v_1v_1} & \cdots & \Gamma_{v_1v_m} \\ \vdots & \ddots & \vdots \\ \Gamma_{v_mv_1} & \cdots & \Gamma_{v_mv_m} \end{bmatrix}_{N_vN_v} \tag{26}$$

where $N_v = m \times n$ and the KLE is known in the following as

$$\Gamma_{vv.vv}\varphi_j - \beta_j\varphi_j = 0 \tag{27}$$

After the truncation the K_vth order according Eq.(18), the KLE representation of *VV* as follows:

$$VV(t,\theta) = \mu_{vv}(t) + \sum_{j=1}^{K_v} \xi_j(\theta)\sqrt{\beta_j}\varphi_j(t) = \mu_{vv} + \sum_{j=1}^{K_v} \xi_j(\theta)X^{(j)}(t) \tag{28}$$

where $\mu_{vv}(t)$ is the vector $X^{(j)}$ rare the KLE vector and $X^{(j)} = \{x_1^{(j)}x_2^{(j)}...x_m^{(j)}\}^T$ with dimension $N_v \times 1$. Thus the component of the $\tilde{v}_i(t,\theta)$ can be:

$$\tilde{v}_i(t,\theta) = \sum_{j=1}^{K_v} \xi_j(\theta)x_i^{(j)}(t) \tag{29}$$

where $x_i^{(j)}(t)$ is of size $1 \times n$ representing the *j*th K-L components of the *j*th term in $V(t,\theta)$, and they can be extracted from the Karhunen-loe've vector $X^{(j)}(t)$according to Eqs.(24)-(28). Subsequently $V(t,\theta)$ becomes

$$V(t,\theta) = \mu_v(t) + \sum_{j=1}^{K_v} \xi_j(\theta)x^{(j)}(t) = \sum_{j=0}^{K_v} \xi_j(\theta)x^{(j)}(t) \tag{30}$$

with the mean vector $\mu_v(t), \xi_0(\theta) = 1, x^{(0)} = \{\overline{v}_1 \overline{v}_2 \ldots \overline{v}_m\}^T$, $x^{(j)}(t) = \{x_1^{(j)} x_2^{(j)} \ldots x_m^{(j)}\}^T$

4. THE ROAD SURFACE ROUGHNESS

The randomness of the surface roughness be represented at a periodic modulated random model. The road surface roughness affects vehicle speed according to the formula between power spectral density (PSD) and PSD [26]. A form of the PSD of roughness is as follows:

$$S_d(h) = S_d(h_0)(h/h_0)^{-\alpha} \tag{31}$$

where h is the spatial frequency in cycle/m and h_0 is the discontinuity frequency equal to $1/2\pi$ (cycle/m). $S_d(h)$ is the PSD in m^3/cycles. $S_d(h_0)$ is the roughness coefficient in m^3/cycles. Eq. (31) assume an estimate of the road roughness by $S_d(h_0)$ value. This classification is done by estimating the constant vehicle speed PSD and taking $\alpha = 2$.

The roughness of the surface in the time domain can be simulated on $S_d(h_0)$ as follows [27].

$$r(x) = \sum_{k=1}^{N} \left(4S_d(h_0) \left(\frac{2\pi k}{L_c h_0} \right)^{-2} \frac{2\pi}{L_c} \right)^{1/2} \cos\left(\frac{2\pi k h_0}{L_c} + \theta_k \right) \tag{32}$$

where L is the double length of the bridge. θ_k is a set of randomly distributed angles between 0 and 2π independently. From formula (32), the roughness samples of the surface can be determined.

5. MOVING LOAD IDENTIFICATION

5.1 Excitation road surface roughness identification using Karhunen-Loe've expansion

From the formula of the Karhunen-Loe've expansion presented in Section 3, with the irregular pavement profiles considered as samples of a Gaussian distribution, the pavement roughness of Eq. (32) can be calculated by its K-L components as follows

$$r(x,\theta) = \sum_{j=1}^{k} \xi_j(\theta) r^{(j)}(x) \tag{33}$$

where $\xi_j(\theta)$ is the variables at orthogonal shown in Eq.(20); θ denotes the random dimension; $r^{(j)}(x)$ is the jth K-L components of the road surface roughness. k is the number of the K-L components for the road surface roughness after truncation.

5.2 Inverse model: moving load identification

The algorithm for identifying moving loads can be constructed according to the model designed in the forward problem. The obtained results of the bridge including displacement, deformation, velocity and acceleration can be applied in the identification of loads. This study, the displacement signals are applied. The displacements below the bridge deck denoted as $\hat{y}(x,t,\psi)$ can be obtained at the deformations from the relationship of the variables as follows

$$\hat{\varepsilon}(x,t,\psi) = -z\frac{\partial^2 \hat{y}(x,t,\psi)}{\partial x^2} \tag{34}$$

where z is the distance at the neutral axis of the beam.

Supposing a set of $\hat{y}(x_i,t_j,\psi_k)$ or $\hat{\varepsilon}(x_i,t_j,\psi_k)$ under the deck is measured, where $k = 1,\ldots N_\psi, i = 1,\ldots,N_m, j = 1,\ldots,N_t$. N_ψ, N_m and N_t are the number of the samples , the measurement points and time instants, respectively. From Eq. (4) (or together with Eq. (34) in case of using deformation), it is possible to obtain the nodal displacement patterns at the degrees of freedom of the elements. The displacement vector of the bridge in the inverse model is known to be $\hat{q}(t,\theta)$ .The dimension of $\hat{q}(t,\theta)$ depends on the number of the points N_m . Assuming the displacement vector $\hat{q}(t,\theta)$ calculated at the measured displacement signal is a multi-dimensional Gaussian process which can be represented by a number of its K-L components from theory introduced as:

$$\hat{q}(t,\theta)=\sum_{j=0}^{\hat{k}_R}\xi_j(\theta)\hat{q}^{(j)}(t) \tag{35}$$

where $\hat{q}^{(j)}(t)=\left\{\hat{q}_1^{(j)}(t)\hat{q}_2^{(j)}(t)...\hat{q}_{N_m}^{(j)}(t)\right\}^T$ is the vector of the *j*th K-L of the measurement displacement samples and $\hat{k}_R$ are denotes KLE components.

The corresponding velocity vectors and acceleration of the displacement denoted as $\dot{\hat{q}}^{(j)}(t)$ and $\ddot{\hat{q}}^{(j)}(t)$ respectively, which can be expressed as

$$\dot{\hat{q}}(t,\theta)=\sum_{j=0}^{\hat{k}_R}\xi_j(\theta)\dot{\hat{q}}^{(j)}(t) \tag{36}$$

$$\dot{\hat{q}}(t,\theta)=\sum_{j=0}^{\hat{k}_R}\xi_j(\theta)\ddot{\hat{q}}^{(j)}(t) \tag{37}$$

where $\dot{\hat{q}}^{(j)}(t)$ and $\ddot{\hat{q}}^{(j)}(t)$ can be obtained at the vector of the KLE component of nodal displacement $\hat{q}^{(j)}(t)$ using the cubic spline technique.

Due to superposition of the linear systems and orthogonal of the KLE components, the random force $\hat{P}(t,\theta)$ can be also represented as

$$\hat{P}(t,\theta)=\sum_{j=0}^{\hat{k}_p}\xi_j(\theta)\hat{P}^{(j)}(t) \tag{38}$$

where $\hat{P}^{(j)}(t)$ is the vector of component of random interaction forces to be identified and $\hat{k}_p=\hat{k}_R$

It can be known that the number of components of the node displacement vectors $\hat{k}_R$ in the inverse model depends on the properties of the displacement of the measurement, the KLE components of the nodal displacements are truncated when the eigenvalue β_n in Eq.(18) is much smaller than the rest.

From Eqs. (35)-(38) into Eq.(8), the equation of motion of the bridge in the inverse problem can be rewritten as:

$$\ddot{\hat{q}}^{(k)}(t)+\hat{C}\dot{\hat{q}}^{(k)}(t)+\hat{K}\hat{q}^{(k)}(t)=\hat{\phi}\hat{P}^{(k)}(t) \tag{39}$$

where $\hat{\phi}$ is the condensed location matrices corresponding to the forces in the inverse model with

$$\hat{\phi}=\left[\hat{\phi}_1\ \hat{\phi}_2\ ...\ \hat{\phi}_n\right]^T \tag{40}$$

with $$\hat{\phi}_1=\frac{2}{\rho L}\sin\frac{\pi vt}{L},\hat{\phi}_2=\frac{2}{\rho L}\sin\frac{2\pi vt}{L},\hat{\phi}_n=\frac{2}{\rho L}\sin\frac{n\pi vt}{L} \tag{41}$$

From Eq.(39), the vector of the interaction forces $\hat{P}^{(k)}(t)$ can be identified as

$$\hat{P}^{(k)}(t)=\left(\hat{\phi}^T\hat{\phi}\right)^{-1}\hat{\phi}^T H^{(k)}(t) \tag{42}$$

where $$H^{(k)}(t)=\ddot{\hat{q}}^{(k)}(t)+\hat{C}\dot{\hat{q}}^{(k)}(t)+\hat{K}\hat{q}^{(k)}(t) \tag{43}$$

5.3 The load identification for vehicle-bridge system based on interval analysis method

In this section, the interval analysis method is presented to determine the bounds of load acting on the uncertain structure.

An *m* dimensional vector λ is used to represent the uncertain parameters that exist in the structural properties problem. An interval variable vector λ^I is used to describe the uncertainty of the parameter λ.

Based on the interval mathematics [28,29] the interval variable vector λ^I can be rewritten in the following form

$$\lambda^I=\left[\lambda^L,\lambda^R\right]=\left[\lambda^c-\lambda^w,\lambda^c+\lambda^w\right]=\lambda^c+\left[-1,1\right]\lambda^w \tag{44}$$

where $\left[\lambda^L, \lambda^R\right]$ denotes an interval, the superscripts L and R represent the lower and upper bounds of the interval respectively. λ^c, λ^w are the midpoint and radius vectors of λ^I, respectively, which are can be expressed as

$$\lambda^c = \frac{\lambda^L + \lambda^R}{2}, \lambda_i^c = \frac{\lambda_i^L + \lambda_i^R}{2}, i = 1, 2, ..., n \tag{45}$$

$$\lambda^w = \frac{\lambda^R - \lambda^L}{2}, \lambda_i^w = \frac{\lambda_i^R - \lambda_i^L}{2}, i = 1, 2, ..., n \tag{46}$$

Based on Eq.(44), the vector λ can be expressed in the following form

$$\lambda = \lambda^c + \delta\lambda \tag{47}$$

$$\delta\lambda \in [-1,1]\lambda^w, \delta\lambda \in [-1,1]\lambda_i^w, i = 1, 2, \ldots, n \tag{48}$$

When the vector λ is described by λ^I for each specific time point t, the load $P(t,\lambda)$ will form a interval vector instead of a real number vector with the respect to the vector λ

$$P(t,\lambda) \in P^I(t) = [P^L(t), P^R(t)] \tag{49}$$

where $P^I(t)$ is the vector of load at the time t and its bounds $P^L(t)$ and $P^R(t)$ can be rewritten as

$$\begin{aligned} P^L(t) &= \min_{\lambda\in\Gamma} P(t,\lambda) \\ P^R(t) &= \max_{\lambda\in\Gamma} P(t,\lambda) \\ \Gamma &= \left\{\lambda \mid \lambda_i^L \le \lambda \le \lambda_i^R\right\}, i = 1, 2, \ldots, n \end{aligned} \tag{50}$$

When a structure contains the parameters λ as introduced in the Section 3, the interval analysis method is applied to the intervals of the force. When the uncertain levels, namely the intervals of parameters with uncertainly are relatively small, the vector $P(t,\lambda)$ in Eq.(49) can be approximated as a function with respect to $\delta\lambda$ the first-order Taylor.

$$P(t,\lambda) = P(t,\lambda^c + \delta\lambda) \approx P(t,\lambda^c) + \sum_{i=1}^{n} \frac{\partial P(t,\lambda^c)}{\partial \lambda_i} \delta\lambda_i \tag{51}$$

From $\delta\lambda$ defined by Eq.(48), the interval vector $P^I(t,\lambda)$ can be obtained through a natural interval extension of Eq.(51) as:

$$P^I(t,\lambda) = P(t,\lambda^c) + \sum_{i=1}^{n} \frac{\partial P(t,\lambda^c)}{\partial \lambda_i} [-1,1]\lambda_i^w \tag{52}$$

So, the lower bounds and the upper bounds of the load at each specific t

$$P^L(t) = \min_{\lambda\in\Gamma} P(t,\lambda) = P(t,\lambda^c) - \sum_{i=1}^{n} \left| \frac{\partial P(t,\lambda^c)}{\partial \lambda_i} \right| \lambda_i^w \tag{53}$$

$$P^R(t) = \max_{\lambda\in\Gamma} P(t,\lambda) = P(t,\lambda^c) + \sum_{i=1}^{n} \left| \frac{\partial P(t,\lambda^c)}{\partial \lambda_i} \right| \lambda_i^w \tag{54}$$

The dynamic load response algorithm in an inverse problem of the system can be formulated based on the excitation force model using KLE combines the interval analysis method. So, from Eqs.(53),(54) into Eq(42)., the lower and upper bounds of the dynamic load of the bridge at each specific time point t can be identified as

$$\hat{P}^{(k)L}(t) = \min_{\lambda\in\Gamma} \hat{P}^{(k)}(t,\lambda) = \left(\hat{\phi}^T\hat{\phi}\right)^{-1} \hat{\phi}^T H^{(k)}(t,\lambda^c) - \sum_{i=1}^{n} \left| \frac{\partial \left(\hat{\phi}^T\hat{\phi}\right)^{-1} \hat{\phi}^T H^{(k)}(t,\lambda^c)}{\partial \lambda_i} \right| \lambda_i^w \tag{55}$$

$$\hat{P}^{(k)R}(t) = \min_{\lambda\in\Gamma} \hat{P}^{(k)}(t,\lambda) = \left(\hat{\phi}^T\hat{\phi}\right)^{-1}\hat{\phi}^T H^{(k)}(t,\lambda^c) + \sum_{i=1}^{n}\left|\frac{\partial\left(\hat{\phi}^T\hat{\phi}\right)^{-1}\hat{\phi}^T H^{(k)}(t,\lambda^c)}{\partial\lambda_i}\right|\lambda_i^w \tag{56}$$

6. NUMERICAL SIMULATION

Axle system is simplified as shown in Fig.1 of the mass-spring bridge model, where the bridge can be reduced to an equivalent stiffness with Euler-Bernoulli beam. The vehicle is studied by a two degrees of freedom of mass-spring. The specific parameters of the bridge - vehicle as: E = 30GPa, I = 3.854m^4, L = 48m, M = 12000kg, m = 500kg, ρ = 8.3x10^{3}kg/m, c_1 = 11593kg/s, k_1 = 28x10^4 N/m, k_2 = 156x10^3 N/m.

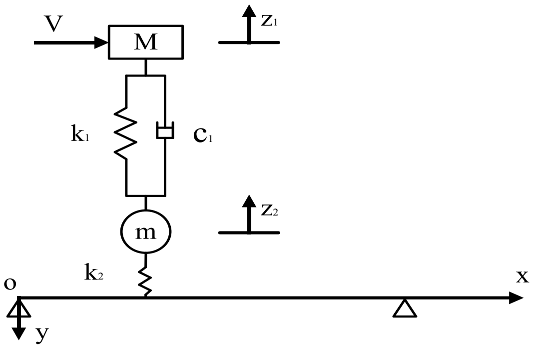

Figure 1: The modal of the vehicle-bridge system

6.1 The road surface roughness

Ten thousand samples of the irregular surface profile are computed through Eq.(32) to represent the process $r(x,\theta)$. This section, the class road $S_d(h_0)$ = 6x10^{-6} m^3/cycles and random angle θ_k is expressed by a random between zero and 2π with the command 'rand'. At an arbitrary position denoted as x_1 on the surface profile along the dimension form a set of samples that will be obtained the corresponding random variable $r(x_1,\theta)$. In the K-L expansion method introduced in Section 5.2, 10,000 samples of the excitation forces $P(t, \theta)$ are obtained from samples of the irregular road profile according to Eq.(3). The KLE is applied to $P(t, \theta)$ and the terms of K–L with the eigenvalue β_j in Eq.(28) which are much smaller than the rest and less than unity, are truncated. The road surface roughness of the vehicle-bridge system is plotted as shown in Fig.2

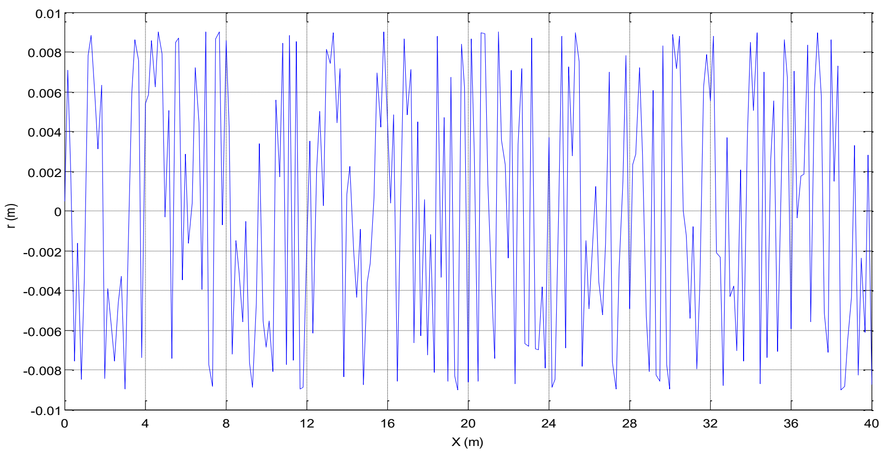

Figure 2: The road surface roughness by KLE method

6.2 Dynamic load identification

In this paper, vehicle speed v = 20 m/s is used to consider dynamic load response. The contact force $P(t)$ between wheel and surface bridge is identified in Eq.(3). The displacement vector of the bridge-vehicle system is computed through the random process road surface roughness $r(x,\theta)$. Displacement response of the bridge at its mid-span can be obtained by Eq. (4) as shown in Fig.3

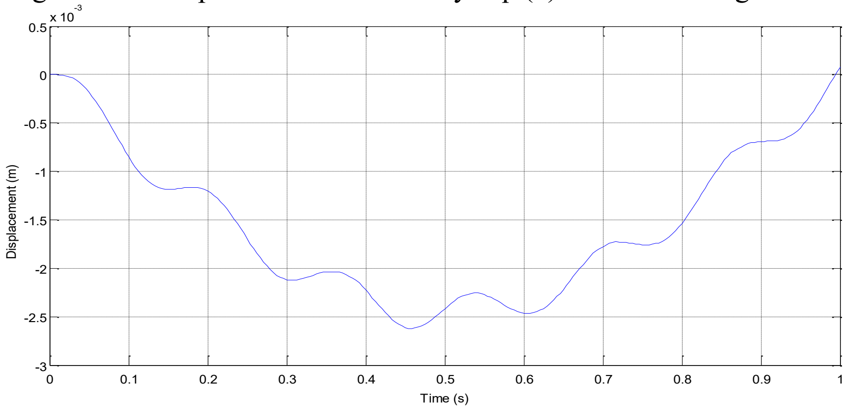

Figure 3: The bridge's displacement at $v = 20$m/s

The Young's modulus E, density ρ, damp coefficient c_1 and stiffness k_1 are treated as uncertain parameters. Uncertainty level of the parameters, namely 5% and 10% off from the midpoints are studied.

The midpoint value of the identified load for all uncertain parameters is computed based on inverse problem in Eqs.(55) or (56) which is obtained by the hybrid method (HKIM) as shown in Fig.4

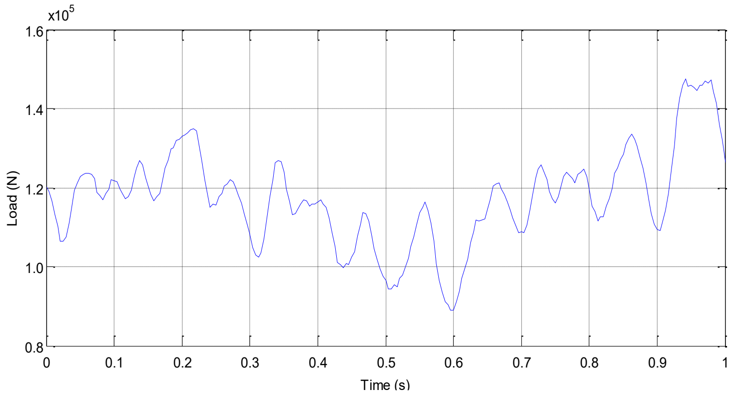

Figure 4: The midpoint of the load at 10% level

The first-order differential coefficients of the load to the parameters E can be calculated according to Eq.(55), (56). The sensitivity curve of the load to interval variable E at each time point t and 10% level are plotted as shown in Figs.(5), respectively. Its can be found that the parameters significant influence to the upper bounds and the lower bounds of the identified load when the sensitivity curves for the parameters are considered.

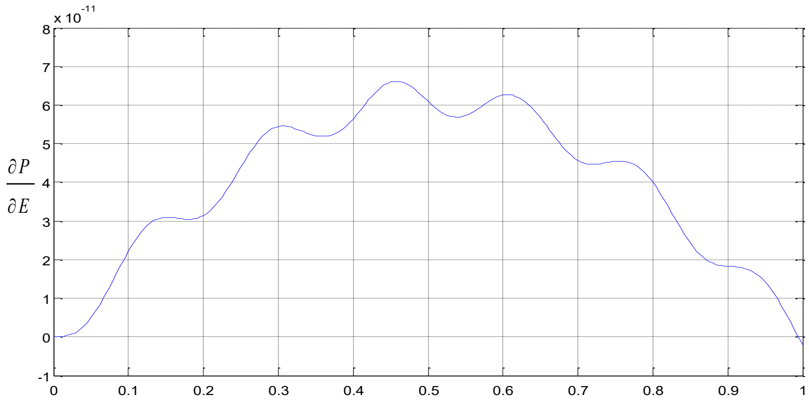

Figure 5: The sensitivity curve of the load to interval variable E

The first-order differential coefficients of the load to the parameters ρ, c_1 and k_1 can be calculated according to Eq.(55), (56). The sensitivity curves of ρ, c_1, k_1 at each time point t and 10% level are plotted as shown in Figs.(6-8), respectively. Its can be found that the parameters significant influence to the upper bounds and the lower bounds of the identified load when the sensitivity curves for the parameters are considered.

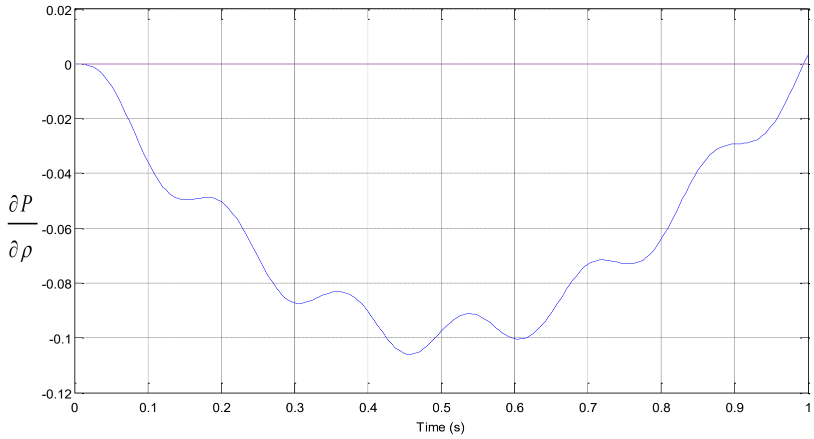

Figure 6: The sensitivity curve to interval variable ρ

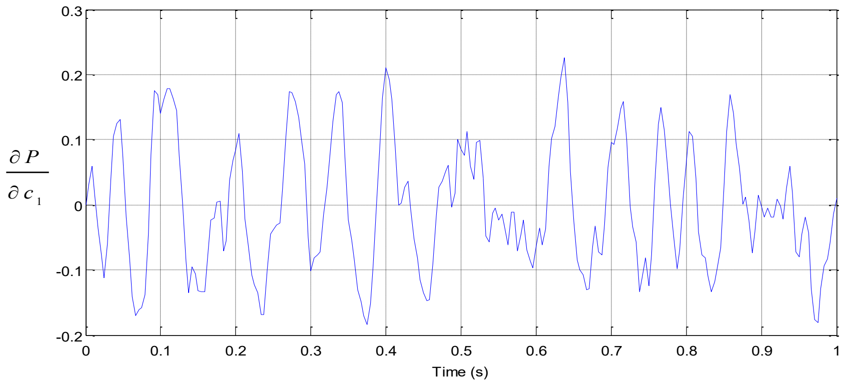

Figure 7: The sensitivity curve to interval variable c_1

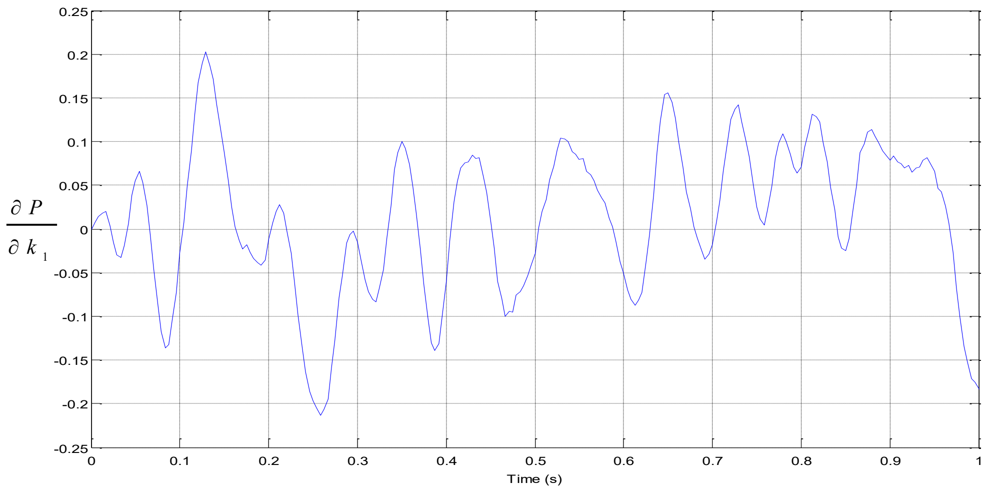

Figure 8: The sensitivity curve to interval variable k_1

To investigate the influences of parameters on the bridge, the uncertainty level of the parameters, namely ± 5% and ± 10% are considered. The lower bounds and the upper bounds of the identified load are computed by Eqs. (55) and Eq. (56) which can be given as shown in Figs.9 and 10, respectively. From Figs.9 and 10, its can be easily observer that when the uncertainty levels of parameters increases, the lower and upper bounds of the identified load increases too. Tables.1 and 2 also show that the load acting bounds on the system are obtained very efficiently for different uncertainty levels.

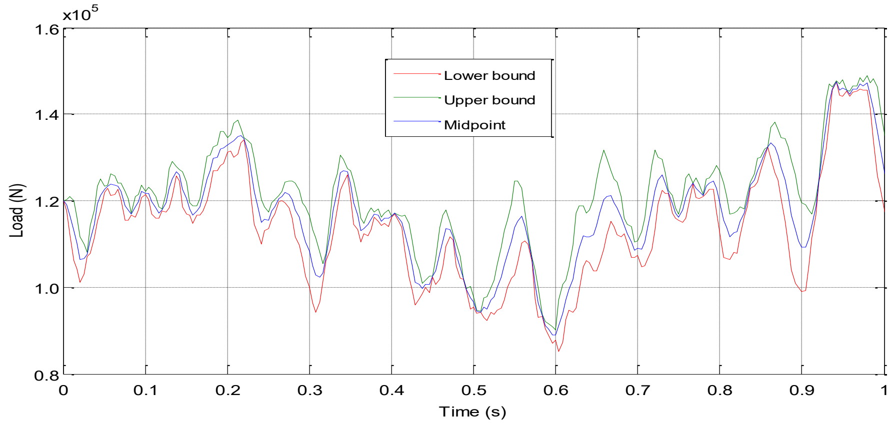

Figure 9: The midpoint and bounds of the load at ± 5% level

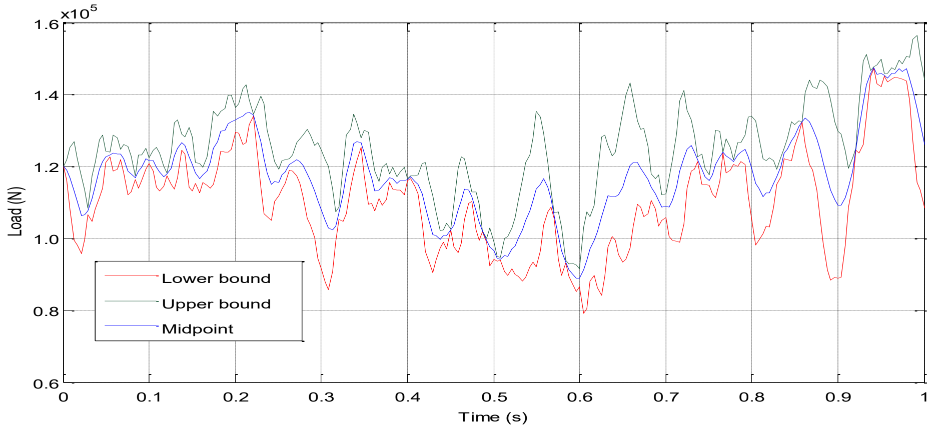

Figure 10: The midpoint and bounds of the load at 10% level

To prove the results obtained by presented method HKIM, the interval analysis method (IAM) is also implemented when the uncertainty levels of all parameters are ± 5% and ± 10% as shown in the Figs.11 and 12 .The results on the upper bounds and the lower bounds of the force at the specific time points by two methods also are listed in Tables.3 and 4. From these tables, they can be obtained that by two methods agree well when the uncertainty level of system parameters are small. The error becomes larger with the increase of uncertainty level of parameters. When uncertainty level is ± 10%, the biggest relative error at 0.4 (s) is 1.9799%.for all system parameters

The Figs.11 and 12 also show that the results calculated by proposed method agree very well with those obtained by using interval analysis method.

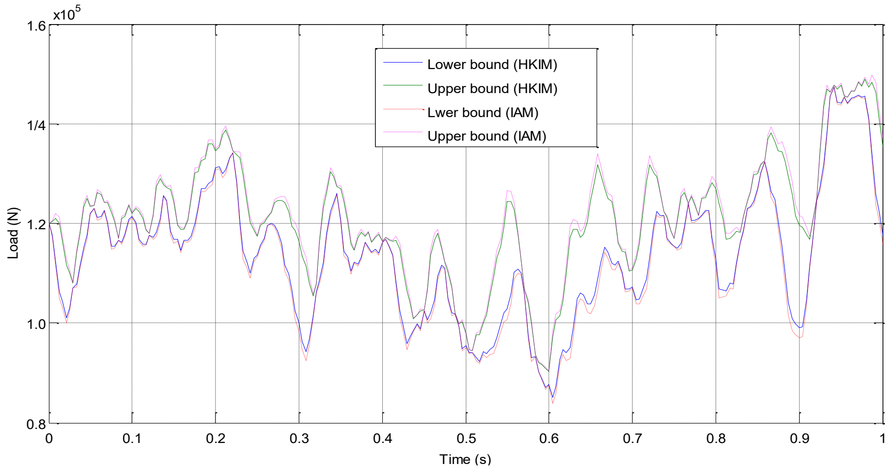

Figure 11: The bounds of the load by HKIM and IAM at ± 5% level

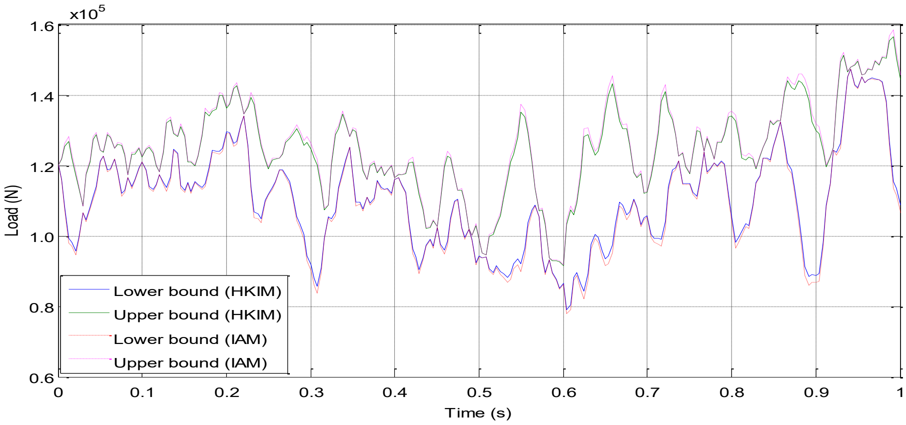

Figure 12: The bounds of the load by HKIM and IAM at ± 10% level

Table 1: The bounds of load by HKIM at ± 5% level

Time(s)	Actual load ($x10^5$)	Vehicle speed v= 20m/s Upper($x10^5$)	Lower($x10^5$)	Deviation (%) Upper	Lower
0.1	1.2127	1.2260	1.2052	1.0967	0.6185
0.2	1.3423	1.3673	1.3212	1.8625	1.5719
0.3	1.0986	1.1656	1.0016	6.0987	8.8294
0.4	1.1735	1.1758	1.1710	0.1960	0.2130
0.5	0.9762	0.9871	0.9518	1.1166	2.4995
0.6	0.9017	0.9226	0.8624	2.3178	4.3629
0.7	1.1003	1.1226	1.0825	2.0267	1.6177
0.8	1.2000	1.2816	1.1137	6.8000	7.1917
0.9	1.1146	1.1986	0.9976	7.5363	10.4970

Table 2: The bounds of load by HKIM at ± 10% level

Time(s)	Actual load($x10^5$)	Vehicle speed v= 20m/s Upper($x10^5$)	Lower($x10^5$)	Deviation (%) Upper	Lower
0.1	1.2127	1.2465	1.2006	2.7872	0.9978
0.2	1.3423	1.3693	1.2954	2.0115	3.4940
0.3	1.0986	1.2516	0.9419	13.9268	14.2636
0.4	1.1735	1.1768	1.1701	0.2812	0.2897
0.5	0.9762	1.0012	0.9418	2.5610	3.5239
0.6	0.9017	0.9426	0.7986	4.5359	11.4340
0.7	1.1003	1.1456	1.0675	4.1171	2.9810
0.8	1.2000	1.3454	1.0997	12.1167	8.3575
0.9	1.1146	1.3016	0.9121	16.7773	18.1680

Table 3: The comparison of results by HKIM and IAM at ± 5% level

	Vehicle speed v= 20m/s					
	Upper bound			Lower bound		
Time (s)	HKAM($x10^5$)	IAM($x10^5$)	Error (%)	HKAM($x10^5$)	IAM($x10^5$)	Error (%)
0.1	1.2260	1.2289	0.2360	1.2052	1.2028	0.1995
0.2	1.3673	1.3885	1.5268	1.3212	1.3102	0.8396
0.3	1.1656	1.1882	1.9020	1.0016	0.9874	1.4381
0.4	1.1758	1.1797	0.3306	1.1710	1.1687	0.1968
0.5	0.9871	1.0018	1.4674	0.9518	0.9446	0.7622
0.6	0.9226	0.9227	0.0108	0.8624	0.8538	1.0026
0.7	1.1226	1.1264	0.3374	1.0825	1.0747	0.7258
0.8	1.2816	1.2979	1.2559	1.1137	1.1076	0.5507
0.9	1.1986	1.2216	1.8828	0.9976	0.9792	1.8791

Table 4: The comparison of results by HKIM and IAM at ± 10% uncertainty level

		Vehicle speed v= 20m/s				
	Upper bound			Lower bound		
Time (s)	HKAM(x10^5)	IAM(x10^5)	Error (%)	HKAM(x10^5)	IAM(x10^5)	Error (%)
0.1	1.2465	1.2492	0.2166	1.2006	1.1972	0.2840
0.2	1.3693	1.3909	1.5774	1.2954	1.2909	0.3486
0.3	1.2516	1.2754	1.9016	0.9419	0.9247	1.8601
0.4	1.1768	1.2001	1.9799	1.1701	1.1656	0.3861
0.5	1.0012	1.0067	0.5493	0.9418	0.9376	0.4480
0.6	0.9426	0.9475	0.5198	0.7986	0.7947	0.4908
0.7	1.1456	1.1496	0.3492	1.0675	1.0612	0.5937
0.8	1.3454	1.3697	1.8062	1.0997	1.0862	1.2438
0.9	1.3016	1.3159	1.0986	0.9121	0.8993	1.4233

7. CONCLUSION

A hybrid method that combines the K-L expansion and interval analysis method is proposed to stably identify the upper bounds, lower bounds of dynamic load acting on the vehicle-bridge system with uncertainty. The vehicle is modeled by a two degrees of freedom mass-spring system and the bridge is modeled as an Euler-Bernoulli beam. Road surface roughness is presented by K-L expansion method and the uncertain parameters of the system are described by the interval. The algorithm of moving force identification can be formulated based on the interval analysis method. The upper and lower bounds of the identified load are computed by the hybrid method HKIM. The results obtained by proposed method HKIM are compared with actual load and interval analysis method IAM. The results obtained by the numerical simulation demonstrate that the proposed method is effective and stable for dynamic load identification of the bridge-vehicle interaction system with uncertainty.

REFERENCES

[1] C. Schenk, L. Bergman, "Response of Continuous System with Stochastically Varying Surface Roughness to Moving Load," *Journal of Engineering Mechanics*, 129(7), 759-768, 2003

[2] T. Xiang, R. Zhao, T. Xu, "Reliability Evaluation of Vehicle–Bridge Dynamic Interaction," *Journal of Structural Engineering*, 133(8), 1092-1099, 2007.

[3] S. S. Law, X. Q. Zhu, "Dynamic behavior of damaged concrete bridge structures under moving vehicular loads," *Engineering Structures*, 26(9), 1279-1293, 2004.

[4] S. S. Law, X. Q. Zhu, "Bridge dynamic responses due to road surface roughness and braking of vehicle," *Journal of Sound and Vibration*, 282(3–5), 805-830, 2005.

[5] C. W. Kim, M. Kawatani, and K. B. Kim, "Three-dimensional dynamic analysis for bridge–vehicle interaction with roadway roughness," *Computers & Structures*, 83(19–20), 1627-1645, 2005.

[6] C. Liu, D. Huang, T. L. Wang, "Analytical dynamic impact study based on correlated road roughness," *Computers & Structures*, 80(20–21), 1639-1650, 2002.

[7] K. Henchi, M. Fafard, M. Talbot, G. Dhatt, "An efficient algorithm for dynamic analysis of bridges under moving vehicles using a coupled modal and physical components approach," *Journal of Sound and Vibration*, 212(4), 663-683, 1998.

[8] S. Y. Lee, S. S. Yhim, "Dynamic behavior of long-span box girder bridges subjected to moving loads: Numerical analysis and experimental verification," *International Journal of Solids and Structures*, 42(18–19), 5021-5035, 2005.

[9] H. S. Zibdeh, "Stochastic vibration of an elastic beam due to random moving loads and deterministic axial forces," *Engineering Structures*, 17(7), 530-535, 1995.

[10] J. G. S. Da Silva, "Dynamical performance of highway bridge decks with irregular pavement surface," *Computers & Structures*, 82(11–12), 871-881, (2004).

[11] S. S. Law, J. Q. Bu, X. Q. Zhu, S. L. Chan, "Vehicle axle loads identification using finite element method," *Engineering Structures*, 26(8), 1143-1153, 2004.

[12] Law, S. S.; Fang, Y. L. (2001). Moving force indentification: optimal state estimation approach. *Journal of Sound and Vibration*, 239(2), 233-254.

[13] Zhu, X. Q.; Law, S. S. (2000). Identification of vehicle axle loads from bridge dynamic responses. *Journal of Sound and Vibration*, 236(4), 705-724.

[14] S. Q. Wu, S. S. Law, "Dynamic analysis of bridge–vehicle system with uncertainties based on the finite element model," *Probabilistic Engineering Mechanics*, 25(4), 425-432, 2010.

[15] C. Jiang, X. Han, F. J. Li, Y. H. Guan, "An uncertain structural optimization method based on nonlinear interval number programming and interval analysis method," *Engineering Structures*, 29(11), 3168-3177, 2007.

[16] C. Jiang, X. Han, G. P. Liu, "Uncertain optimization of composite laminated plates using a nonlinear interval number programming method," *Computers & Structures*, 86(17–18), 1696-1703, 2008.

[17] C. Jiang, X. Han, G. R. Liu, "Optimization of structures with uncertain constraints based on convex model and satisfaction degree of interval," *Computer Methods in Applied Mechanics and Engineering*, 196(49–52), 4791-4800, 2007.

[18] C. Jiang, X. Han, G. R. Liu, G. P. Liu, "A nonlinear interval number programming method for uncertain optimization problems," *European Journal of Operational Research*, 188(1), 1-13, 2008.

[19] C. Jiang, G. R. Liu, and X. Han, "A Novel Method for Uncertainty Inverse Problems and Application to Material Characterization of Composites," *Experimental Mechanics*, 48(4), 539-548, 2008.

[20] J. Liu, X. Han, H. M. Ning, Y. C. Bai, "Dynamic load identification for uncertain structures based on interval analysis and regularization method," *International Journal of Computational Methods* 08(04), 667-683, 2011.

[21] G. R. Liu, W. B. Ma, X. Han, "An inverse procedure for identification of loads on composite laminates," *Composites Part B: Engineering*, 33(6), 425-432, 2002.

[22] N. Liu, W. Gao, C. Song, N. Zhang, Y. L. Pi, "Interval dynamic response analysis of vehicle-bridge interaction system with uncertainty," *Journal of Sound and Vibration*, 332(13), 3218-3231, 2013.

[23] N. Liu, W. Gao. C. M. Song, N. Zhang, "Hybrid probabilistic interval dynamic analysis of vehicle–bridge interaction system with uncertainties," *Int. J. Str. Stab. Dyn*, 14(03), 25, 2014.

[24] L. Yu, H. T. Chan, "Recent research on identification of moving loads on bridges," *Journal of Sound and Vibration,* 305(1-2), 3021, 2007.

[25] R. Ghanem, P. Spanos, "Spectral Stochastic Finite-Element Formulation for Reliability Analysis," *Journal of Engineering Mechanics*, 117(10), 2351-2372, 1991.

[26] P. Andren, "Power spectral density approximations of longitudinal road profiles," *International Journal of Vehicle Design*, 40(1), 2-14, 2006.

[27] K. Henchi, M. Fafard, M.Talbot, and G. Dhatt, "An efficient algorithm for dynamic analysis of bridges under moving vehicles using a coupled modal and physical components approach." *Journal of Sound and Vibration*, Vol. 212, Issue 4, pp. 663-83, 1998.

[28] G. R. Liu, X. Han, "Computational Inverse Technique in Nondestructive Evaluation," *CRC Press, ISBN*, 0849315239, 2003.

[29] Z. Qiu, X. Wang, "Comparison of dynamic response of structures with uncertain-but-bounded parameters using non-probabilistic interval analysis method and probabilistic approach," *International Journal of Solids and Structures*, 40(20), 5423-5439, 2003.

[30] N. Liu, W. Gao, C. Song, and N. Zhang, "Hybrid probabilistic interval dynamic analysis of vehicle–bridge interaction system with uncertainties", *International Journal of Structural Stability and Dynamics*, Vol. 14, No. 03, 1350069 (2014).

[31] *Nengguang Liu, Wei Gao, Chongmin Song , Nong Zhang , Yong-Lin Pi,* Interval dynamic response analysis of vehicle-bridge interaction system with uncertainty*, Journal of Sound and Vibration, Vol332, Issue 13, 24 June 2013.*

[32] *Pinghe Ni, Jun Li, Hong Hao, Hongyuan Zhou,* Reliability based design optimization of bridges considering bridge-vehicle interaction by Kriging surrogate model, *Engineering Structures, Volume 246, 1 November 2021.*